

Inhalational Delivery of β -glucan-chitosan-poly(lactic co-glycolic) acid Nanoparticles Enhance Alveolar Macrophage Rifampin Concentrations for the Treatment of Tuberculosis

Hilliard L. Kutscher, Maria Tamblin, Shanta Karki, Lee Chaves, Marissa Baird, Afrin Parvin, Evon Smith, Admire Dube, Zhaoqi Zhang, Saptarshi Chakraborty, Patrick Kenney, and Jessica L. Reynolds*

Despite multiple treatments for tuberculosis (TB), there are ≈ 10 million new cases and 1.5 million deaths annually, warranting the need for new therapeutics. Major clinical treatment issues include the length of treatment which is associated with patient non-compliance; and poor cellular drug penetration leading to the generation of drug-resistant strains. This study underscores the potential of β -glucan-chitosan (CS) poly(lactic co-glycolic) acid (PLGA) nanoparticles as a promising immunostimulatory adjunct for TB treatment. To facilitate drug delivery to alveolar macrophage, a CS-PLGA nanoparticle is developed containing rifampin in the core with β -glucan as a surface ligand, to stimulate the immune system. Mice are administered a single dose of nanoparticles or free rifampin by oropharyngeal aspiration. Pharmacokinetic investigations reveal sustained release properties of rifampin in vivo, extending over a week. Furthermore, comprehensive analysis indicates stimulation of the innate immune system, as evidenced by cytokine profiling, while concurrently revealing no detrimental effects on the alveolar epithelium, as indicated by histological examination and albumin lung leak assessment. These findings collectively establish a strong foundation for the development of a novel adjuvant immunotherapy approach for TB.

1. Introduction

Prior to the Covid-19 pandemic, tuberculosis (TB), caused by *Mycobacterium tuberculosis* (*Mtb*), was the leading cause of death from a single infectious agent.^[1,2] TB is also the leading cause of death from patients who have HIV, and the TB and HIV epidemics have co-evolved.^[3] TB is more prominent in resource-limited settings and spreads via aerosolization. Small-molecule therapeutic cocktails have been used since the 1950s to treat patients.^[4] However, their long treatment times (up to 9 months) and side effects caused by systemic toxicity have led to poor patient compliance resulting in multi-drug resistance (MDR-TB). The 4-drug fixed dose standard of care therapy (ethambutol, pyrazinamide, isoniazid, and rifampin (HREZ)) has been used for decades, and recently new drug regimens including bedaquiline, pretomanid, and linezolid (BPaL) have been added to the clinician's toolbox.^[5,6] However,

H. L. Kutscher
Institute for Lasers
Photonics and Biophotonics
The State University of New York at Buffalo
Buffalo, NY 14260, USA

H. L. Kutscher
Department of Anesthesiology
The State University of New York at Buffalo
Buffalo, NY 14203, USA

H. L. Kutscher, M. Tamblin, S. Karki, L. Chaves, M. Baird, A. Parvin,
E. Smith, J. L. Reynolds
Division of Allergy
Immunology
and Rheumatology Department of Medicine
Clinical Translational Research Center
The State University of New York at Buffalo
Buffalo, NY 14203, USA
E-mail: jl8@buffalo.edu

A. Dube
Pharmaceutics at the School of Pharmacy
University of the Western Cape (UWC)
Robert Sobukwe Road, Bellville 7535, South Africa

Z. Zhang, S. Chakraborty
Department of Biostatistics
The State University of New York at Buffalo
Buffalo, NY 14203, USA

 The ORCID identification number(s) for the author(s) of this article can be found under <https://doi.org/10.1002/adtp.202400057>

DOI: 10.1002/adtp.202400057

these small molecules are administered systemically, resulting in the potential for side effects and drug-drug interactions. To overcome these challenges, new therapeutic modalities need to be explored.

We propose immune stimulation of alveolar macrophage, the predominant site of *Mtb* infection, while concomitantly delivering an anti-TB therapeutic using an immunostimulatory nanoparticle. We developed a core-shell (core: poly(lactic-co-glycolic) acid [PLGA]; shell: chitosan [CS]) nanoparticle that stimulates macrophage and delivers rifampin (Rif),^[7,8] a model rifamycin drug used in TB therapy that suffers from a short half-life (poor pharmacokinetics) and long length of therapy (often 9 months).^[9] Immune stimulation is induced by surface coating the nanoparticle with 1,3- β -glucan (β -glucan), a polysaccharide found on the surface of yeast that binds the Dectin-1 receptor on macrophage.^[7,8,10–12] β -glucan's interaction with Dectin-1 induces phagocytosis and T-cell differentiation.^[10] Previous in vitro studies using this immunostimulatory nanoparticle found enhanced immune activation and increased intracellular uptake of Rif.^[7,8] We recently demonstrated inhibition of colony forming units (CFU) formation in vitro in *Mtb*-infected macrophage using an immunostimulatory nanoparticle.^[12] It is important to note that other laboratories have shown that β -glucan incubated with *Mtb* infected macrophage significantly reduces the number of CFU, which is attributed to immune stimulation of the macrophage.^[13] Intraperitoneal injection of β -glucan significantly lowers *Mtb* burden in the lung in a mouse model of *Mtb*.^[14] These findings support evidence of immune stimulation as a method for the clearance of pathogens and lay the groundwork for additional testing of this immunostimulatory nanoparticle therapy.

Various strategies have been explored to enhance TB treatment, particularly through the utilization of the biocompatible and biodegradable polymer PLGA in the synthesis of nanoparticles (Reviewed by Shao et al, 2022^[15]). Clinical trials of PLGA-formulated drugs have demonstrated that PLGA has low toxic side effects associated with it. Studies have shown that PLGA protects drugs from enzymatic degradation and offers stability.^[16] Rifamycin-loaded PLGA nanoparticles have been dosed orally in humans^[17] and mice^[18] or by IV administration,^[19] and were larger in size^[20] or targeted to macrophage using lactate.^[19] In each case, these PLGA formulations have outperformed free Rif alone, however none have combined an immune stimulatory agent (1,3- β -glucan) and been dosed by oropharyngeal aspiration (OPA), which mimics inhalation and would be the intended route of administration. For example, rifapentine-loaded PLGA nanoparticles have been shown to be more effective against *Mtb* than free rifapentine.^[18] These findings not only emphasize the crucial role of PLGA as a carrier for TB drugs but also highlight its potential to transform TB treatment strategies. Incorporating immune-stimulatory agents on the surface of PLGA nanoparticles and utilizing OPA for drug administration could further en-

hance therapeutic outcomes by leveraging the host immune response against *Mtb*.

For effective *Mtb* eradication, high drug concentrations at early time points following drug administration are required within the macrophage, and these high concentrations need to be maintained over long periods.^[21] This is therefore the intracellular pharmacokinetic (PK) goal of effective TB drug therapy. Against this backdrop, we propose macrophage targeted immune stimulating nanoparticles as a drug delivery system for optimal increased intracellular TB drug exposure. However little information is known about the in vivo PK and pharmacodynamics (PD) of this immunostimulatory nanoparticle when dosed by inhalation. Therefore, the goal of this study was to determine the PK and PD of this immune stimulatory nanoparticle and its safety profile in healthy mice. The proposed studies are intended to provide a proof of principle upon which a novel immunotherapeutic approach will be optimized for in vivo macrophage-targeted drug delivery and immune stimulation.

Our PK studies demonstrate after a single OPA dose of nanoparticles to healthy mice, the intended clinical route of administration, Rif was detected in the cellular fraction of the BAL up to 7 days post-dosing. This demonstrates sustained release properties in vivo over 1 week. Furthermore, we found stimulation of the innate immune system (cytokine analysis) and no damage to the alveolar epithelium (histology and albumin analysis).

2. Experimental Section

2.1. Materials

Poly(lactic-co-glycolic) acid (PLGA, 50:50 ester terminated 24–38 kDa MW), chitosan oligosaccharide lactate (CS, 5 kDa MW), 1,3- β -glucan (β -glucan), polyvinyl alcohol (PVA, Molviol 4–88, 31 kDa MW), and rifapentine (RIFP) were purchased from Millipore-Sigma (St. Louis, MO). Methylene chloride (ACS reagent grade, $\geq 99.5\%$), and acetonitrile were purchased from Fisher Scientific. Rifampin ($>98\%$) (Rif) was purchased from TCI America (Portland, OR). All materials were used as received. Kollisolv PYR was a generous gift from BASF Corp. (Florham Park, NJ).

2.2. Synthesis of β -Glucan-CS-PLGA Nanoparticles

β -glucan-CS-PLGA (β -C-P) nanoparticles (Table 1) containing Rif were prepared via a water/oil/water emulsion, followed by solvent evaporation. The initial water/oil emulsion was formed through probe sonication (1 min at 21% power; Cole Parmer, Vernon Hills, IL) with 20 mg of PLGA and 4 mg of Rif in 500 μ L methylene chloride and 100 μ L distilled water. The CS coating was achieved through subsequent probe sonication (1 min at 21% power) of the initial water/oil emulsion combined with 500 μ L of a second water phase containing 1.2 mg mL⁻¹ CS, 20 mg mL⁻¹ PVA, 0.02 M NaCH₃COO buffer pH 4.4. The buffer was used to protonate CS and to facilitate electrostatic attachment of CS to the negative surface of the non-coated PLGA nanoparticles. CS-PLGA nanoparticles were formed upon evaporation of methylene

P. Kenney
Adult and Pediatric Infectious Disease
The State University of New York at Buffalo
Buffalo, NY 14203, USA

Table 1. Dosage table for nanoparticle administration.

Label	% Nanoparticle Solids [w/v]	PLGA [mg k ⁻¹ g]	Surface β -glucan [ng/mg PLGA]	Rifampin [mg k ⁻¹ g]
Rif alone	-	-	-	4.33
20% C-P	20% Solids (no β -glucan)	333	-	4.33
20% β -C-P	20% Solids	333	25	4.33
10% β -C-P	10% Solids	166.5	25	2.17
5% β -C-P	5% Solids	83.25	25	1.08

Nanoparticle concentrations of PLGA, β -glucan, and Rif in a single bolus dose depending on the percentage of nanoparticle solids administered by OPA. Note: 20% solids = 200 mg mL⁻¹ PLGA = 10 mg PLGA/50 μ L dose = 333 mg PLGA/kg body weight = 4.33 mg Rif/kg.

chloride through overnight stirring in a 1-dram vial. The resulting nanoparticles were collected by centrifugation at 16000 x g for 10 min. The pellet was washed twice with distilled water to remove excess surfactant and non-encapsulated Rif, followed by resuspension to 100 mg mL⁻¹ PLGA in either 0.5x PBS (CS-PLGA nanoparticles: C-P) or 2.5 μ g mL⁻¹ β -glucan in 2.5 mM NaOH and 0.5x PBS (β -glucan-CS-PLGA nanoparticles: β -C-P) using a bath sonicator. The nanoparticles were collected by centrifugation at 16000 x g for 10 min, decanted, and resuspended using a bath sonicator to a final concentration of 200 mg mL⁻¹ PLGA in PBS for immediate use.^[8] The content of surface β -glucan by electrostatic binding was determined using a GlucateLL kit (Associate of Cape Cod, East Falmouth, MA).^[22] The resulting nanoparticles are referred to as: C-P and β -C-P (Table 1). In a separate set of experiments for intracellular uptake, Nile Red (Millipore Sigma, St. Louis, MO) was encapsulated in the PLGA core instead of Rif.

2.3. Nanoparticle Characterization

The hydrodynamic diameter and surface charge of resulting C-P and β -C-P nanoparticles were determined using dynamic light scattering (DLS) and Zeta potential analysis performed on an SZ-100 Nanopartica (Horiba Instruments, Inc. Irvine, CA). To prepare samples for testing, 2 μ L of the nanoparticle dispersion was added to 1 mL DI water. Scanning electron microscopy (SEM) was used to confirm the size of the nanoparticles, as well as observe any change to surface structure following coating. For these experiments, the final suspension of nanoparticles was in H₂O instead of PBS. A 10 μ L drop of 20 mg mL⁻¹ nanoparticles was added to a glass slide and allowed to dry under vacuum followed by coating with evaporated carbon, using a high vacuum evaporator (Denton 502 Evaporator, Denton Vacuum, LLC, Moorestown, NJ, USA). The samples were imaged using a field emission SEM (Hitachi SU-70, Tokyo, Japan) at 2.0 keV as shown in Figure S1 (Supporting Information).

2.4. Rifampin (Rif) Concentration Determination

The amount of Rif in the C-P and β -C-P nanoparticles was determined using a Nanodrop 2000 measured at 338 nm blanked against acetonitrile with a quadratic standard curve from 2.5 to 250 μ g mL⁻¹ ($R^2 = 0.9919$). Nanoparticles were dissolved 1:40 in acetonitrile and bath sonicated.

2.5. Animals

Male and female CD-1 mice 4–6 weeks old (20–24 g) were purchased from Charles Rivers Laboratories (Wilmington, MA) and housed under a 12 h normal phase light-dark cycle. Drinking water and food were freely available. All procedures involving animals were reviewed and approved by the Institutional Animal Care and Use Committee of the University at Buffalo.

2.6. Oropharyngeal Aspiration (OPA) and Oral Gavage

Briefly, mice were anesthetized using 5% isoflurane, and body temperature was maintained on a water-circulating heating pad. The mouse was hung from its superior incisors, followed by the tongue being extended using forceps. A 50 μ L bolus dose of nanoparticles or vehicle was administered to the back of the throat, and the mouse inhaled the liquid resulting in delivery to the lungs. The mouse was returned to its cage and observed until it regains consciousness.^[23] The dose of nanoparticles or Rif alone given is shown in Table 1. For oral gavage, mice were administered a 50 μ L bolus dose of Rif (2.5 mg mL⁻¹ in 2.5% (v/v) KollosoLV PYR in PBS using a 20 Ga feeding tube (Instech, Plymouth Meeting, PA).

2.7. Serum and Bronchoalveolar Lavage (BAL) Collection

Briefly, mice were anesthetized using 5% isoflurane and maintained on a water circulating heating pad. Using a 5.5 mm lancet, a sub-mandibular puncture was used to collect blood. Mice were then returned to the anesthetic chamber followed by cervical dislocation. BAL was performed using two 5 mL syringes connected to a 3-way stopcock, where 1 syringe is empty, and the other contains 5 mL of saline, and connected to the intra-tracheal catheter (20Gx1 Surflo, Terumo) secured with 1-0 braided silk suture.^[23] The collected BAL was weighed and placed on ice. To recover the cells in the BAL, samples were centrifuged at 500 x g for 10 min at 4 °C. The cell-free BAL supernatants were stored at -221280 °C.^[12,23] To the cell pellet, 40 μ L of acetonitrile was added and store at -0 °C until HPLC quantitation. BAL fluid cytology showed $\geq 97\%$ macrophage by cytology (See Figure S1, Supporting Information).

2.8. Rif Concentration in BAL Cells as Determined by HPLC

Rif detection was performed on a Shimadzu LC20 series with Xbridge phenyl 3.5 μ m 2.1x100 mm column (Waters Corp.,

Milford, MA) and detected by UV-vis at 338 nm or by MS MRM (Rif 823.56→791.37; rifapentine IS 877.67→845.4) using an API2000 triple-quadrupole mass spectrometer. The final sample matrix was 1.5:1.5:1 MeOH:ACN:H₂O containing 0.5 mg mL⁻¹ ascorbic acid and 5 µg mL⁻¹ RIFP (IS). Samples were briefly vortexed and sonicated, then centrifuged at 4 °C for 15 min at 16000 × g. The supernatant was transferred to an HPLC vial with an insert for injection. The injection volume was 2 µL for HPLC/MS and 10 µL for HPLC/UV-vis. The flow rate was 0.2 mL min⁻¹ with the following gradient: Time 0 min: 35%B, Time 4 min: 80%B, Time 7 min: 80%B, Time 7.1 min: 35%B Time 12 min: 35%B. Mobile phase A: 0.05% ammonium formate pH 3, Mobile phase B: acetonitrile. Standard curve was quadratic from 5–1250 ng mL⁻¹ for MS detection or linear from 0.1–100 µg mL⁻¹ for UV-vis detection.

2.9. Cytokine ELISA

BAL supernatants were analyzed for TNF α , IL-6, IL-1 β , IL-12 and IFN- γ using mouse DuoSet ELISA kits, according to the manufacturer's instructions (R&D systems Cat. #: DY410, DY406, DY401, DY419, and DY485). Assay detection lower limits were: 31.2 pg mL⁻¹ for TNF α , 15.6 pg mL⁻¹ for IL-6, 15.6 pg mL⁻¹ for IL-1 β , 39.1 pg mL⁻¹ for IL-12 and 31.2 pg mL⁻¹ for IFN- γ . Briefly, the respective capture antibody was diluted to the working concentration and used to coat a 96-well microplate that was incubated overnight at room temperature (RT). The 96-well microplate was washed 3 times followed by blocking with Reagent Diluent followed by incubation for 1 h at RT. The 96-well microplate was washed 3 times. A standard curve in the range of 0 pg to 2000pg mL⁻¹ of the recombinant murine cytokine was generated. 100 µL⁻¹ of standards or unknowns were added to each well and incubated for 2 h at RT. The plates were washed and the Detection Antibody at the working concentration was added to each well and incubated for 2 h at RT. The plate was washed and 100 µL⁻¹ 1X Streptavidin-HRP solution was added to each well and incubated for 20 min at RT. The plates were washed and 100 µL stabilized chromogen was added to each well and incubated for 30 min at RT in the dark. 50 µL of Stop Solution was added to each well. The plates were read at 450 nm using a BioTek Synergy LX multimode reader (BioTek-Agilent).

2.10. Albumin ELISA

BAL supernatants were analyzed for albumin using an ELISA kit according to the manufacturer's instructions (Mouse Albumin ELISA Kit (ab108791), Abcam, Waltham, MA). Briefly, an albumin standard curve in the range of 0 to 100 µg mL⁻¹ was generated. 25 µL of standards or unknown samples were added to each well followed by the addition of 25 µL of 1X Biotinylated Albumin to each well and incubated for 1 h at RT. The plate was washed 5 times with 1X Wash Buffer followed by the addition of 50 µL of 1X SP Conjugate to each well and incubated for 30 min. The plate was washed 5 times and then 50 µL of Chromogen Substrate was added per well and incubated for 30 min. 50 µL of Stop Solution was added to each well and the plate was then immediately read at 450 nm.

2.11. Recovery of Lung and Spleen

Mice were euthanized at various timepoints after OPA by cervical dislocation under 5% isoflurane anesthesia. Mice were pinned to a surgical board and a suture loop was placed around the incisors of the mouse and pinned to secure the head. The mouse was dissected to expose the thoracic cavity and neck. Lung and spleen were dissected out, weighed, and placed in a 15 mL centrifuge tube on ice until further processing described below.^[12,23]

2.12. Lung Histology

Lungs were submerged in 10% buffered formalin in a volume at least 20 times that of the specimen for a minimum of 24 h. Samples were placed in cassettes followed by serial washing with 70%, 95%, and 100% ethanol. The fixed tissue was embedded in paraffin via dehydration and clearing. Paraffin blocks were cut into 5 µm sections using a microtome. Tissue sections were stained with H&E and visualized under a microscope (Revolve Microscope, Echo BICO Company, San Diego).

2.13. Lung Disassociation and Antibody Staining

For every 50 mg of tissue collected, 1 mL of cold Hanks Balanced Salt Solution (HBSS) containing 11 ng mL⁻¹ DNase I and 2.5 µg mL⁻¹ Collagenase Type IV was added to a C-tube. Tissue was digested using a Miltenyi GentleMACS Octo Disassociator using the factory "37 mLDK" setting. After the cycle was complete, C-tubes were centrifuged at 300 × g for 5 min, the cell suspension was transferred to a new tube. Red blood cell lysis was done by adding 40 µL of ACK lysis buffer to each tube, followed by a 10 min incubation period, followed by centrifugation at 300 × g for 5 min. Samples were strained into a new tube with a 40 µm strainer. Samples were centrifuged for 5 min at 300 × g. Liquid was aspirated off the pellet and 600 µL⁻¹ of FACS buffer was used to resuspend the sample pellets. FC Blocker was added to each tube then incubated 5 min before antibodies were added. A master mix of thirteen antibodies was prepared to be added to each tube for staining. The antibodies used to stain the cells of the lung were from Biolegend [Ly6C (PerCp-Cy5.5) (B363119), CD8 (PE-TXRd) (B365389), CD4 (PE-Cy5) (B313577), DEC205 (PE-Cy7) (B350425), CD 45 (A700) (B369737), CD 14 (APC-Cy7) (B298317), CD5 (BV421) (B312475), CD11b (BV510) (B360991), MCHII (BV650) (B349777), CD11c (BV711) (B347781), CD19 (BV785) (B360776), Siglec-F (BV605) (2343438), and F4/F80 (APC) (3602239)]. Once the antibodies were added, the sample was left on ice and covered for 20 min. Stained samples were then centrifuged at 300 × g for 5 min, aspirated, and resuspended with 600 µL⁻¹ of FACS buffer. Samples were analyzed on a BD LSR-Fortessa Flow Cytometer; data analysis was done using FlowJo (BD Biosciences).

2.14. Spleen Disassociation

For disassociation, 3 mL of HBSS was added to each tube to resuspend the spleen. The spleen was strained through a 40 µm

strainer by mechanical disassociation using the end of a 3 mL syringe. The pellet was collected by centrifugation for 5 min 300 × g, with the supernatant being aspirated. Red blood cell lysis was performed using 300 μL of ACK lysis buffer for 10 min followed by centrifugation for 5 min at 300 × g, with supernatant subsequently aspirated. 800 μL of FACS buffer was added to each tube and the pellet was resuspended then transferred to a flow tube for staining of the immune cells. FC Blocker was added to each flow tube for 5 min prior to antibodies. The antibodies to stain the cells of the spleen were from Biolegend [Ly6C (PerCp-Cy5.5) (B363119), CD8 (PE-TXRd) (B365389), CD4 (PE-Cy5) (B313577), CD5 (BV421) (B312475), CD11b (BV510) (B360991), and CD19 (BV785) (B369776)]. The samples were then covered and incubated for 20 min. Samples were analyzed on a BD LSR-Fortessa Flow Cytometer; data analysis was done using FlowJo (BD Biosciences).

2.15. Statistical Analysis

2.15.1. PK and AUC

AUC was computed using the R package *PK*.^[24] One-way ANOVA was performed using GraphPad Prism, version 9.3.1 (GraphPad Software, San Diego, CA) followed by Tukey correction for multiple comparisons. Data shown represent mean ± SEM; *n* = 9–16.

2.15.2. Cell Populations by Flow cytometry and Albumin ELISA

Analysis was performed using GraphPad Prism, version 9.3.1 (GraphPad Software, San Diego, CA). For comparisons of every mean to a control mean, statistical analysis was done using ordinary two-way ANOVA followed by Dunnett's multiple comparisons test. Data shown represent mean ± SEM, *n* = 8.

2.15.3. Intracellular Uptake Determined by Flow Cytometry

Statistical analysis was done one-way ANOVA followed by Tukey's multiple comparisons test. Data shown represent mean ± SEM, *n* = 8.

2.15.4. Cytokine Secretion

The concentration of cytokines in the BAL supernatant from mice that received OPA of PBS was compared to control mice that did not receive OPA using a one-way ANOVA followed by Tukey's multiple comparisons test. No significant changes were observed between these two groups; therefore, control and OPA of PBS data are combined and are represented as PBS. Experimental groups (20% β-C-P, 10% β-C-P, 5% β-C-P, 20% C-P or Rif alone) were compared to PBS at respective time points (2 to 168 h). Cytokines from C-P or Rif alone at 72–168 h were below the detection limit of ELISA and are recorded as not-detectable (ND). A separate gamma (log link) generalized linear mixed effects model for each experimental setting was considered. The animal-specific cytokine concentration observed at

each time point and from a treatment/PBS was considered as the response variable, and fixed effect terms for all linear interactions of treatments (including PBS) and the time points were considered. A separate random effect intercept term was considered for each animal to formally acknowledge within-versus-between animal variations. A full Bayesian estimation of the models for principled and stable statistical inference within the current modeling framework, rigorously acknowledging the relatively larger number of model parameters compared to the sample sizes^[25] was considered. A weakly informative default independent normal (mean = 0, sd = 2.5) priors for the fixed effect coefficients for *scaled* explanatory variables following^[26] was utilized. Probabilistic programming language stan (via its R interface package *rstanarm*) Markov chain Monte Carlo (MCMC) based posterior computations (4 independent MCMC chains, each ran for 1000 warmup and 1000 final iterations) was used. From the fitted models, the average effect ratios of the form mean (treatment)/mean (PBS) computed separately for each time point (and also averaged across all time points) and mean (time point)/mean (2 h) was computed separately for each treatment/PBS (and also averaged across all treatments/PBS). These effect ratios were subsequently inferred through their point and interval estimates based on the posterior median and 95% equal-tailed intervals. Statistical significance was measured at the 95% posterior probability level: an effect ratio with 95% posterior probability excluding the value of 1 was deemed statistically significant. All computations including data pre-processing and post-processing of MCMC results were done in R and stan using R packages *tidyverse*,^[27] *rstanarm*,^[26] and *marginal effects*.^[28] Data shown represent mean ± SEM, *n* = 4 to 12.

2.16. Ethical Statement

All procedures involving animals were reviewed and approved by the Institutional Animal Care and Use Committee of the University at Buffalo

3. Results

β-C-P nanoparticles encapsulating Rif were an average size of 235 nm and +12.47 mV charge. Figure S1 (Supporting Information) shows representative images of all nanoparticles by SEM. Data demonstrate nanoparticles are similar in size and surface morphology.

3.1. Single Dose PK

Data shown in Figure 1A–D demonstrate that the nanoparticle formulations deliver significantly higher amounts of Rif than Rif alone in the BAL (Table 2A), and that there is rapid clearance from 2–24 h. Rif concentration in BAL of mice receiving Rif alone was found to be in the ng/mL quantities, requiring HPLC/MS detection (Figure 1A,B). Furthermore, Rif remained present in the lung for all nanoparticle formulations for at least 7 days (Figure 1C,D), compared < ≈8 h for Rif alone, whereas the nanoparticle serum Rif concentration (Figure 1E,F) and total exposure (Table 2A) are significantly less than systemic Rif dosed by

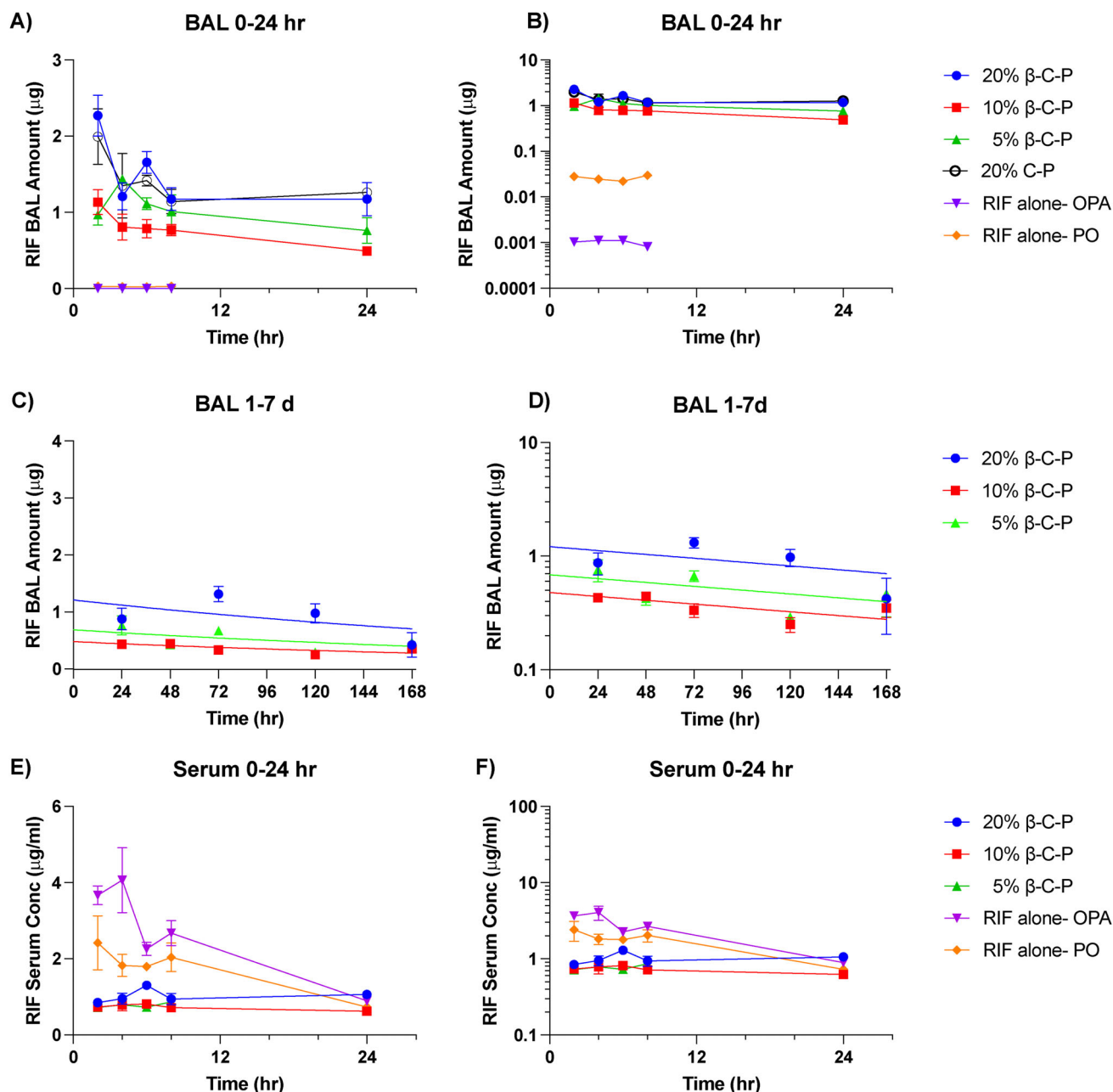


Figure 1. Time course of Rif in serum and BAL cell pellet after administration by OPA or oral gavage. A,B) Amount of Rif recovered in BAL cell pellet over 24 h. C,D) Amount of Rif recovered in BAL cell pellet over 1 week. Terminal phase fit using a 1 phase PK model. A shared terminal slope was the preferred model. E,F) Serum concentration of Rif over 24 h. Data shown represent mean \pm SEM; $n = 4-8$. PO = oral gavage; OPA = oropharyngeal aspiration. B,D,F) Semi-log plot of A, C, E, respectively.

oral gavage and OPA. In addition, while the minimal inhibitory concentration (MIC) of Rif in serum is 1 to 5 $\mu\text{g mL}^{-1}$,^[9] at all-time points measured and all doses of nanoparticles (20% β -C-P, 10% β -C-P, 5% β -C-P, 20% C-P) the detected Rif concentration in the serum is greater than 0.6 $\mu\text{g mL}^{-1}$.

We determined the $\text{AUC}_{2-8\text{h}}$ using the PK package of R. This time frame was chosen because BAL and serum concentrations were below the limit of detection after 8 h for many groups, and earlier timepoints would be necessary to bet-

ter understand the absorptive phase. The AUC of 20% β -C-P nanoparticles in the BAL is significantly higher (9.75 ± 0.595 vs 0.151 ± 0.004 $\mu\text{g}\times\text{h}$; mean \pm SEM) than free drug gavage (current route of Rif administration) but is significantly lower (6.3 ± 0.338 vs 11.69 ± 1.02 $\mu\text{g mL}^{-1}\times\text{h}$; mean \pm SEM) in the serum (Table 2).

Finally, the terminal slope of Rif from the BAL was similar between 20% β -C-P, 10% β -C-P, and 5% β -C-P indicating that the elimination mechanism is not saturated at this PLGA

Table 2. AUC 2–8 h estimates of Rif in BAL (A) and serum (B).

A)								
BAL	AUC _{2,8h} estimate $\mu\text{g}^*\text{h}$	SEM	n	Adjusted P value, comparison to				
				Rif alone PO	Rif alone OPA	20% C-P	20% β -C-P	10% β -C-P
Rif alone PO	0.151	0.004	9	–				
Rif alone OPA	0.006	0	16	$p = 0.9994$	–			
20% C-P	8.66	0.946	16	$p < 0.0001$	$p < 0.0001$	–		
20% β -C-P	9.75	0.595	16	$p < 0.0001$	$p < 0.0001$	$p = 0.6923$	–	
10% β -C-P	5.09	0.45	16	$p < 0.0001$	$p < 0.0001$	$p < 0.0001$	$p < 0.0001$	–
5% β -C-P	7.08	0.312	16	$p < 0.0001$	$p < 0.0001$	$p = 0.2915$	$p = 0.0076$	$p = 0.0947$
B)								
Serum	AUC _{2,8h} estimate $\mu\text{g}/\text{mL}^*\text{h}$	SEM	n	Adjusted p value, comparison to				
				Rif alone PO	Rif alone OPA	20% β -C-P	10% β -C-P	
Rif alone PO	11.69	1.02	16	–				
Rif alone OPA	18.98	1.78	16	$p < 0.0001$	–			
20% β -C-P	6.3	0.338	16	$p = 0.0035$	$p < 0.0001$	–		
10% β -C-P	4.66	0.319	9	$p = 0.0010$	$p < 0.0001$	$p = 0.8695$	–	
5% β -C-P	4.62	0.135	11	$p = 0.0004$	$p < 0.0001$	$p = 0.8299$	$p = 0.99$	

PO = oral gavage; OPA = oropharyngeal aspiration. Comparison by one-way ANOVA with Tukey post-hoc correction.

concentration (Figure 1C,D). Based on the available data and using noncompartmental PK analysis, the presence of β -glucan does not alter the terminal clearance, and there is rapid clearance from 2–24 h.

3.2. Cytokine Secretion in BAL post-OPA of Nanoparticles

Data shown in Table 3 represent TNF α secretion in the BAL supernatant 2 to 168 h post OPA of 20% β -C-P, 10% β -C-P, 5% β -C-P, 20% C-P or Rif alone. 20% β -C-P, 10% β -C-P, or 5% β -C-P induced a significant increase in the concentration of TNF α secretion from 2 to 168 h post OPA compared to PBS. The highest concentration of TNF α secretion induced by 20% and 10% β -C-P was at 2 h, while the highest concentration of TNF α secretion induced by 5% β -C-P was at 6 h. 20% C-P significantly decreased the concentration of TNF α at 2, 8, 24 and 48 h post-OPA.

Data shown in Table 4 represent IL-6 secretion in the BAL supernatant 2 to 168 h post OPA of 20% β -C-P, 10% β -C-P, 5% β -C-P, 20% C-P or Rif alone. 20% β -C-P, 10% β -C-P, or 5% β -C-P induced a significant increase in the concentration of IL-6 secretion from 2 to 168 h post OPA compared to PBS. 20% C-P or Rif alone had no effect on IL-6 secretion at all times studied.

Data shown in Table 5 represent IL-1 β secretion in the BAL supernatant 2 to 168 h post-OPA of 20% β -C-P, 10% β -C-P, 5% β -C-P, 20% C-P or Rif alone. 20% β -C-P induced a significant increase in the concentration of IL-1 β secretion from 2 to 168 h post-OPA compared to PBS. 10% β -C-P induced a significant increase in the concentration of IL-1 β secretion from 2 to 48 h post-

OPA compared to PBS. 5% β -C-P induced a significant increase in the concentration of IL-1 β secretion from 2 to 6 h post-OPA compared to PBS. 20% C-P or Rif alone had no effect on IL-1 β secretion.

3.3. Concentration of Albumin in BAL

Data shown in Figure 2 demonstrates no significant change in the concentration of albumin in the BAL supernatant following a single bolus OPA dose of Rif alone, 20% C-P, 20% β -C-P, 10% β -C-P, or 5% β -C-P at 2 to 168 h post-OPA compared to PBS. These data indicate no damage to the alveolar epithelium.

3.4. Immune Cell Populations in the Lung Following Nanoparticle Exposure

The cell populations analyzed in the lung following a single bolus OPA dose of Rif alone, 20% C-P, 20% β -C-P, 10% β -C-P, or 5% β -C-P were total immune cells (CD45), T-cells (CD5), B-cells (CD19), alveolar macrophage (F4/80, CD11c), and neutrophils (CD11b, Ly6c). Data shown in Figure 3a demonstrates the CD45+ immune cell population in the lung. 20% β -C-P, 10% β -C-P, 5% β -C-P, 20% C-P or Rif alone had no effect on the CD45+ cell population compared to PBS. Figure 3b demonstrates the CD5+ T-cell population following OPA of 2 to 168 h post OPA of 20% β -C-P, 10% β -C-P, 5% β -C-P, 20% C-P or Rif alone. There was a significant increase in the CD5+ T-cell population at 48 h post-

Table 3. Effect of nanoparticle exposure on TNF α secretion in the BAL supernatant.

Concentration of TNF α [pg/mL] in BAL supernatant post-OPA							
Time [h]	Comparison	Mean	SEM	Estimate	Conf. low	Conf. high	Significance
2	PBS	43.22	11.12	–	–	–	–
	PBS vs 20% β -C-P	2127.00	123.31	48.32	29.18	81.02	Y
	PBS vs 10% β -C-P	1484.11	187.56	34.34	19.16	65.61	Y
	PBS vs 5% β -C-P	891.02	18.87	20.56	11.52	39.15	Y
	PBS vs 20% C-P	5.33	0.73	0.12	0.07	0.24	Y
4	PBS vs RIF alone	110.94	13.86	2.48	1.46	4.14	Y
	PBS	64.91	18.94	–	–	–	–
	PBS vs 20% β -C-P	3246.65	120.01	50.19	29.99	82.29	Y
	PBS vs 10% β -C-P	2439.06	69.55	38.17	21.63	71.01	Y
	PBS vs 5% β -C-P	1425.30	86.76	22.26	12.36	40.69	Y
6	PBS vs 20% C-P	70.60	10.91	1.11	0.62	2.09	N
	PBS vs RIF alone	99.29	12.41	1.47	0.89	2.46	N
	PBS	63.00	15.23	–	–	–	–
	PBS vs 20% β -C-P	1680.65	92.69	27.04	16.62	43.75	Y
	PBS vs 10% β -C-P	2305.03	248.25	37.01	21.09	70.19	Y
8	PBS vs 5% β -C-P	1987.95	85.10	32.1	18.1	61.33	Y
	PBS vs 20% C-P	41.17	2.05	0.67	0.37	1.2	N
	PBS vs RIF alone	90.39	11.30	1.42	0.86	2.34	N
	PBS	97.24	7.42	–	–	–	–
	PBS vs 20% β -C-P	1231.40	72.14	12.56	7.72	20.76	Y
24	PBS vs 10% β -C-P	1772.29	134.71	18.31	10.11	33.99	Y
	PBS vs 5% β -C-P	743.76	49.72	7.69	4.33	14.36	Y
	PBS vs 20% C-P	6.98	1.06	0.07	0.04	0.13	Y
	PBS vs RIF alone	116.73	14.59	1.05	0.64	1.72	N
	PBS	59.82	16.35	–	–	–	–
48	PBS vs 20% β -C-P	451.70	12.41	7.61	4.42	13.17	Y
	PBS vs 10% β -C-P	330.39	12.79	5.65	2.98	11	Y
	PBS vs 5% β -C-P	241.99	27.85	4.08	2.2	7.77	Y
	PBS vs 20% C-P	19.66	0.71	0.33	0.18	0.65	Y
	PBS vs RIF alone	117.43	14.68	1.79	1.03	3.19	Y
72	PBS	39.91	5.56	–	–	–	–
	PBS vs 20% β -C-P	310.05	11.12	22.81	12.65	41.46	Y
	PBS vs 10% β -C-P	284.20	16.08	7.65	4.09	14.78	Y
	PBS vs 5% β -C-P	188.68	10.53	5.21	2.65	9.93	Y
	PBS vs 20% C-P	8.45	0.92	0.23	0.12	0.44	Y
120	PBS vs RIF alone	60.40	12.67	1.22	0.82	1.8	N
	PBS	31.3	4.12	–	–	–	–
	PBS vs 20% β -C-P	270.65	20.39	10.01	5.56	18.04	Y
	PBS vs 10% β -C-P	216.19	18.33	8.08	4.26	15.63	Y
	PBS vs 5% β -C-P	275.49	26.63	10.35	5.52	19.39	Y
120	PBS vs 20% C-P	ND	–	–	–	–	–
	PBS vs RIF alone	ND	–	–	–	–	–
	PBS	51.63	8.99	–	–	–	–
	PBS vs 20% β -C-P	109.62	1.50	2.13	1.19	3.8	Y
	PBS vs 10% β -C-P	285.23	38.25	5.47	2.89	10.53	Y
120	PBS vs 5% β -C-P	281.99	19.48	5.51	2.82	10.7	Y
	PBS vs 20% C-P	ND	–	–	–	–	–
	PBS vs RIF alone	ND	–	–	–	–	–

(Continued)

Table 3. (Continued)

Concentration of TNF α [pg/mL] in BAL supernatant post-OPA							
Time [h]	Comparison	Mean	SEM	Estimate	Conf. low	Conf. high	Significance
168	PBS	39.26	13.72	–	–	–	–
	PBS vs 20% β -C-P	101.79	1.40	3.17	1.8	5.36	Y
	PBS vs 10% β -C-P	528.72	76.77	13.6	7.32	25.76	Y
	PBS vs 5% β -C-P	312.24	42.52	8.1	4.47	15.03	Y
	PBS vs 20% C-P	ND	–	–	–	–	–
	PBS vs RIF alone	ND	–	–	–	–	–

A single bolus dose (50 μ L) was administered to mice of either 20% β -C-P, 10% β -C-P, 5% β -C-P, 20% C-P or Rif alone by OPA. BAL was performed and BAL supernatant was analyzed for TNF α secretion using an ELISA. Data shown represent the mean \pm SEM; ($n = 4$ to 12). The average effect ratios of the form mean (treatment)/mean (PBS) computed separately for each time was computed separately for each treatment/PBS (and also averaged across all treatments/PBS). These effect ratios were subsequently inferred through their point and interval estimates based on the posterior median and 95% equal-tailed intervals. Statistical significance was measured at the 95% posterior probability level: an effect ratio with 95% posterior probability excluding the value of 1 was deemed statistically significant.

OPA for both 20% β -C-P ($10.41\% \pm 1.5$, $p < 0.05$) and 10% β -C-P ($14.23\% \pm 4.5$, $p < 0.0001$) compared to PBS ($2.14\% \pm 0.8$). Figure 3c demonstrates the B cell population in the lung. At 24 h, compared to PBS ($16.17\% \pm 3.06$), 10% β -C-P ($6.96\% \pm 2.4$, $p < 0.05$) significantly decreased the B cell population in the lung. Figure 3d demonstrates the alveolar macrophage population (CD11c and F4/80, SiglecF and DEC205) following OPA of 2 to 168 h post OPA of 20% β -C-P, 10% β -C-P, 5% β -C-P, 20% C-P or Rif alone. There was a significant increase the alveolar macrophage population with 20% β -C-P ($10.37\% \pm 1.67$, $p < 0.05$), 5% β -C-P ($12.10\% \pm 1.55$, $p < 0.05$) and Rif alone ($13.05\% \pm 2.06$, $p < 0.05$) compared to PBS ($3.12\% \pm 0.537$ at 24 h post-OPA. 20% β -C-P ($16.24\% \pm 1.25$, $p < 0.001$), 10% β -C-P ($17.95\% \pm 1.39$, $p < 0.0001$) and Rif alone ($17.06\% \pm 0.89$, $p < 0.0001$) compared to PBS ($3.95\% \pm 0.79$) at 48 h. At 7 days post OPA, 20% β -C-P ($30.37\% \pm 7.7$, $p < 0.0001$), 10% β -C-P ($33.75\% \pm 0.49$, $p < 0.0001$), 5% β -C-P ($32.47\% \pm 0.98$, $p < 0.0001$) and Rif alone ($33.1\% \pm 1.6$, $p < 0.0001$) significantly increased the alveolar macrophage population compared to PBS ($6.53\% \pm 2.23$). Figure 3e demonstrates the proinflammatory macrophage population (F4/80, CD14, and CD11b, non-tissue resident macrophage) in the lung. 20% β -C-P, 10% β -C-P, 5% β -C-P, 20% C-P or Rif alone had no effect on the proinflammatory macrophage population compared to PBS. Figure 3f demonstrates the neutrophil population (CD11b+, Ly6c^{low}) following OPA with PBS, 20% β -C-P, 10% β -C-P, 5% β -C-P, 20% C-P or Rif alone. A significant increase in the neutrophil population occurred at 24 h with 10% β -C-P ($14.1\% \pm 4.73$, $p < 0.0001$) compared to PBS ($1.017\% \pm 0.11$) and at 48 h following 20% β -C-P ($19.37\% \pm 4.72$, $p < 0.0001$) and 10% β -C-P (15.02 ± 3.47 , $p < 0.0001$) administration compared to respective PBS ($0.94\% \pm 0.13$).

3.5. Immune Cell Populations in the Spleen Following Nanoparticle Exposure

The cell populations in the spleen that were analyzed following a single bolus OPA dose of Rif alone, 20% C-P, 20% β -C-P, 10% β -C-P, or 5% β -C-P were T-cells (CD5), B-cells (CD19), macrophage (CD11c), and neutrophils (CD11b, Ly6c). Data shown in Figure 4a

demonstrates the T-cell population in the spleen. 20% β -C-P ($2.63\% \pm 0.40$, $p < 0.0003$), 10% β -C-P ($3.37\% \pm 1.46$, $p < 0.0002$), 5% β -C-P ($4.75\% \pm 0.345$, $p < 0.006$), and Rif alone ($3.37\% \pm 0.22$, $p < 0.0001$) decreased the T-cell population in the spleen at 24 h post OPA compared to PBS. This effect on the T-cell population is also present at 168 h post-OPA which includes 20% β -C-P ($1.33\% \pm 0.17$, $p < 0.01$), 10% β -C-P ($0.80\% \pm 0.15$, $p < 0.004$), 5% β -C-P ($1.65\% \pm 0.24$, $p < 0.02$), and Rif alone ($1.26\% \pm 0.18$, $p < 0.01$). 5% β -C-P decreased the T-cell population at 48 h ($2.23\% \pm 0.172$, $p < 0.022$) and 72 h ($1.81\% \pm 0.683$, $p < 0.016$) post-OPA while Rif alone ($1.26\% \pm 0.184$, $p < 0.022$) decreased the T-cell population at 72 h as well. Data shown in Figure 4b demonstrates the B cell population in the spleen. 20% β -C-P, 10% β -C-P, 5% β -C-P, 20% C-P or Rif alone had no effect on the B cell population compared to PBS. Data shown in Figure 4c demonstrates the macrophage population (CD11c+) in the spleen. At 168 h 20% β -C-P ($9.29\% \pm 0.87$, $p < 0.01$) increased the population compared to PBS. 20% C-P increased the macrophage population at 24 h ($12.76\% \pm 2.74$, $p < 0.0001$) and 48 h ($11.70\% \pm 2.68$, $p < 0.004$) post-OPA. The macrophage population decreased with Rif alone at 72 h ($2.74\% \pm 0.62$, $p < 0.004$). Figure 4d demonstrates the neutrophil population (CD11b and Ly6c) in the spleen. There was increase in the neutrophil population from 48 h ($4.29\% \pm 0.61$, $p < 0.04$), 72 h ($5.98\% \pm 1.07$, $p < 0.02$), and 168 h ($5.64\% \pm 0.58$, $p < 0.02$) with 5% β -C-P compared to PBS. 20% β -C-P ($6.39\% \pm 0.918$, $p < 0.04$) increased neutrophils at 72 h and 10% β -C-P ($7.15\% \pm 0.613$, $p < 0.0003$) increased neutrophils at 168 h compared to PBS.

3.6. Histology

Data shown in Figure S2 (Supporting Information), demonstrate representative H&E-stained lung sections following 2 to 168 h post-OPA. Images demonstrate normally preserved parenchyma following a single bolus OPA dose of Rif alone, 20% C-P, 20% β -C-P, 10% β -C-P, or 5% β -C-P.

3.7. Intracellular Uptake in Alveolar Macrophage

Data shown in Figure S3 (Supporting Information) demonstrates intracellular uptake in alveolar macrophage 30 min to 12 h

Table 4. Effect of nanoparticle exposure on IL-6 secretion in the BAL supernatant.

Concentration of IL-6 (pg/ml) in BAL supernatant post-OPA							
Time (h)	Comparison	Mean	SEM	estimate	Conf. low	Conf. high	Significance
2	PBS	35.53	1.75	–	–	–	–
	PBS vs 20% β -C-P	225.16	4.61	6.60	5.03	8.57	Y
	PBS vs 10% β -C-P	179.93	9.14	5.22	3.75	7.27	Y
	PBS vs 5% β -C-P	155.94	3.58	4.58	3.26	6.42	Y
	PBS vs 20% C-P	27.36	1.96	0.78	0.56	1.09	N
4	PBS vs RIF alone	53.42	2.08	1.53	1.16	1.98	N
	PBS	45.05	2.78	–	–	–	–
	PBS vs 20% β -C-P	193.96	4.44	4.53	3.50	5.82	Y
	PBS vs 10% β -C-P	156.13	8.95	3.59	2.57	4.94	Y
	PBS vs 5% β -C-P	138.13	3.16	3.21	2.31	4.43	Y
6	PBS vs 20% C-P	46.01	2.75	1.05	0.76	1.46	N
	PBS vs RIF alone	57.26	1.85	1.31	1.00	1.70	N
	PBS	41.67	2.30	–	–	–	–
	PBS vs 20% β -C-P	181.51	1.80	4.57	3.51	5.99	Y
	PBS vs 10% β -C-P	155.94	6.16	3.91	2.81	5.43	Y
8	PBS vs 5% β -C-P	133.50	2.91	3.38	2.42	4.71	Y
	PBS vs 20% C-P	52.10	4.29	1.28	0.92	1.78	N
	PBS vs RIF alone	64.92	1.49	1.63	1.26	2.17	N
	PBS	40.22	2.65	–	–	–	–
	PBS vs 20% β -C-P	135.24	1.77	3.59	2.74	4.66	Y
24	PBS vs 10% β -C-P	163.15	5.02	4.37	3.12	6.10	Y
	PBS vs 5% β -C-P	137.48	2.47	3.67	2.63	5.09	Y
	PBS vs 20% C-P	40.20	2.86	1.05	0.76	1.45	N
	PBS vs RIF alone	55.24	1.66	1.46	1.09	1.92	N
	PBS	49.31	2.27	–	–	–	–
48	PBS vs 20% β -C-P	151.94	1.82	3.17	2.42	4.13	Y
	PBS vs 10% β -C-P	143.10	6.87	2.98	2.12	4.16	Y
	PBS vs 5% β -C-P	138.54	2.58	2.90	2.12	4.00	Y
	PBS vs 20% C-P	46.44	3.20	0.98	0.71	1.38	N
	PBS vs RIF alone	55.29	0.98	1.15	0.87	1.53	N
72	PBS	25.21	0.73	–	–	–	–
	PBS vs 20% β -C-P	149.49	1.60	5.49	4.20	7.09	Y
	PBS vs 10% β -C-P	168.87	5.68	6.22	4.47	8.64	Y
	PBS vs 5% β -C-P	154.47	1.64	5.70	4.09	7.97	Y
	PBS vs 20% C-P	26.99	2.36	0.96	0.69	1.34	N
120	PBS vs RIF alone	58.34	2.25	2.10	1.61	2.75	N
	PBS	27.79	0.93	6.87	–	–	–
	PBS vs 20% β -C-P	172.14	2.32	7.47	5.33	10.29	Y
	PBS vs 10% β -C-P	186.86	7.25	6.73	4.81	9.23	Y
	PBS vs 5% β -C-P	167.37	5.75	1.05	0.76	1.47	Y
120	PBS vs 20% C-P	ND	–	–	–	–	–
	PBS vs RIF alone	ND	–	–	–	–	–
	PBS	29.61	1.04	–	–	–	–
	PBS vs 20% β -C-P	240.86	5.51	8.20	6.27	10.68	Y
	PBS vs 10% β -C-P	177.77	7.42	6.09	4.48	8.52	Y
120	PBS vs 5% β -C-P	135.11	3.69	4.64	3.37	6.40	Y
	PBS vs 20% C-P	ND	–	–	–	–	–
	PBS vs RIF alone	ND	–	–	–	–	–

(Continued)

Table 4. (Continued)

Concentration of IL-6 (pg/ml) in BAL supernatant post-OPA							
Time (h)	Comparison	Mean	SEM	estimate	Conf. low	Conf. high	Significance
168	PBS	34.26	0.91	–	–	–	–
	PBS vs 20% β -C-P	264.58	10.36	7.68	5.72	10.22	Y
	PBS vs 10% β -C-P	124.94	3.35	3.63	2.61	5.09	Y
	PBS vs 5% β -C-P	135.04	1.86	3.93	2.80	5.50	Y
	PBS vs 20% C-P	ND	–	–	–	–	–
	PBS vs RIF alone	ND	–	–	–	–	–

A single bolus dose (50 μ L) was administered to mice of either 20% β -C-P, 10% β -C-P, 5% β -C-P, 20% C-P or Rif alone by OPA. BAL was performed and BAL supernatant was analyzed for IL-6 secretion using an ELISA. Data shown represent the mean \pm SEM; ($n = 4$ to 12). The average effect ratios of the form mean (treatment)/mean (PBS) computed separately for each time was computed separately for each treatment/PBS (and also averaged across all treatments/PBS). These effect ratios were subsequently inferred through their point and interval estimates based on the posterior median and 95% equal-tailed intervals. Statistical significance was measured at the 95% posterior probability level: an effect ratio with 95% posterior probability excluding the value of 1 was deemed statistically significant.

post-OPA. Data demonstrate that nanoparticles are within alveolar macrophage post OPA.

4. Discussion

Most notably, our investigation revealed that incorporating the immune stimulatory agent 1,3- β -glucan on the surface of the nanoparticle led to the stimulation of the immune system specific to the lung milieu in healthy mice. Following a single OPA administration of these nanoparticles, we observed cytokine secretion and innate and adaptive cell recruitment without any discernible damage to the alveolar epithelium, as indicated by histological assessments and albumin levels. Our PK studies elucidate that following a single OPA administration of nanoparticles, mimicking the intended clinical route for Rif delivery, the drug remained detectable in the cellular fraction of the BAL up to 7 days post-dosing. This underscores the sustained release characteristics of the formulation in vivo, spanning a duration of 1 week. These findings collectively underscore the potential of this formulation not only for immune stimulation and prolonged drug release but also for its benign impact on the pulmonary microenvironment, offering promising prospects for therapeutic applications.

PLGA nanoparticles have emerged as a promising platform for delivering drugs for TB treatment.^[29] PLGA nanoparticles can encapsulate TB drugs, providing a controlled and sustained release of the therapeutic agents over an extended period.^[30] This sustained release helps maintain effective drug concentrations at the site of infection, which is crucial for combating TB.^[29] PLGA nanoparticles can be designed to target specific cells or tissues.^[7,8,12,31] Existing literature supports the use of PLGA nanoparticles or microparticles for the delivery of TB therapeutics. For example, rifamycin loaded PLGA nanoparticles have been dosed orally in humans^[17] or mice^[18] or by IV administration,^[19] were larger in size^[20] or targeted to macrophage using lactate.^[19] In each case, these PLGA formulations have outperformed Rif alone, however none have combined an immune stimulatory agent (1,3- β -glucan) with OPA, which mimics inhalation and would be the intended route of administration. For example, rifapentine-loaded PLGA nanoparticles have been shown to be more effective against *Mtb* than

free rifapentine.^[18] While existing literature reports the superiority of PLGA formulations over Rif alone, our investigation introduces a novel dimension by incorporating an immune stimulatory agent, namely 1,3- β -glucan, on the surface of the PLGA nanoparticle. This particular ligand, 1,3- β -glucan, was selected on its potential to inhibit *Mtb*. Studies have demonstrated that microgram concentrations of β -glucan led to a reduction in *Mtb* H37Rv survival within peritoneal macrophages of BALB/c mice, with particulate β -glucan exhibiting greater efficacy than its soluble counterpart.^[13] In a separate study, mice receiving intraperitoneal injections of β -glucan exhibited a significantly lower *Mtb* burden in the lungs compared to those administered PBS.^[14] However, Betz et al. observed that microgram concentrations of insoluble whole glucan microparticles and a soluble glucan extract did not reduce intracellular *Mtb* growth in macrophages.^[32] Previous studies including our own have also utilized β -glucan as a targeting ligand or formulated as nanoparticles for TB therapy. Tukulula et al, demonstrated that conjugation of PLGA nanoparticles with 1,3- β -glucan increased intracellular Rif in macrophages.^[31] Our laboratory demonstrated an increased uptake of Rif when delivered through β -glucan-CS-PLGA nanoparticles in macrophage, compared to free drug. Furthermore, nanoparticles containing surface β -glucan ligands exhibited a higher uptake rate than those without the ligand, indicating enhanced phagocytic activity of the cells. Measurements taken after 24 h (in vitro) revealed higher intracellular concentrations of Rif in cells treated with the nanoparticle compared to those treated solely with the antibiotic.^[7,8] Additional efficacy studies showed a significant reduction in intracellular accumulation of *Mtb* in monocyte-derived macrophages (MDM) incubated with β -glucan-CS-PLGA nanoparticles^[12] further supporting its role as an anti-TB therapeutic drug delivery vehicle.

The overall goal of this study was to determine the in vivo PK of an immunostimulatory nanoparticle in healthy mice. While multiple different types of TB therapeutics can be encapsulated within this nanoparticle, for this study we chose Rif as our model rifamycin drug. The rifamycin drug class includes Rif, rifabutin, and rifapentine. These drugs have low cellular drug diffusion, and their low intracellular concentrations are rapidly cleared from macrophage which plays a role in the duration of treatment and development of drug-resistant strains.^[9] Rif is a hydrophobic

Table 5. Effect of nanoparticle exposure on IL-1 β secretion in the BAL supernatant.

Concentration of IL-1 β [pg/ml] in BAL supernatant post-OPA							
Time (h)	Comparison	Mean	SEM	estimate	conf. low	conf. high	Significance
2	PBS	42.44	1.51	–	–	–	–
	PBS vs 20% β -C-P	193.62	9.75	4.49	3.18	6.31	Y
	PBS vs 10% β -C-P	143.88	2.83	3.36	2.38	4.64	Y
	PBS vs 5% β -C-P	73.35	3.18	1.72	1.17	2.56	Y
	PBS vs 20% C-P	51.39	1.25	1.20	0.81	1.78	N
4	PBS	49.54	3.61	1.16	0.77	1.73	N
	PBS	34.88	2.33	–	–	–	–
	PBS vs 20% β -C-P	227.92	3.57	6.51	4.67	9.05	Y
	PBS vs 10% β -C-P	155.84	3.68	4.45	3.18	6.24	Y
	PBS vs 5% β -C-P	78.82	1.37	2.26	1.51	3.37	Y
6	PBS vs 20% C-P	46.27	1.15	1.33	0.91	1.93	N
	PBS vs RIF alone	50.19	3.32	1.43	0.98	2.11	N
	PBS	32.83	2.07	–	–	–	–
	PBS vs 20% β -C-P	156.19	5.83	4.73	3.31	6.63	Y
	PBS vs 10% β -C-P	155.84	3.68	3.08	2.19	4.33	Y
8	PBS vs 5% β -C-P	55.87	2.29	1.71	1.15	2.5	Y
	PBS vs 20% C-P	52.15	5.46	1.58	1.06	2.36	N
	PBS vs RIF alone	44.67	2.33	1.35	0.91	2.01	N
	PBS	37.30	1.17	–	–	–	–
	PBS vs 20% β -C-P	112.38	2.18	3	2.14	4.16	Y
24	PBS vs 10% β -C-P	155.84	3.68	1.84	1.29	2.54	Y
	PBS vs 5% β -C-P	54.40	1.93	1.09	0.74	1.62	N
	PBS vs 20% C-P	54.24	3.73	1.45	0.99	2.11	N
	PBS vs RIF alone	46.56	3.18	1.24	0.85	1.81	N
	PBS	40.63	1.85	–	–	–	–
48	PBS vs 20% β -C-P	80.35	1.41	1.98	1.41	2.76	Y
	PBS vs 10% β -C-P	64.07	2.37	1.58	1.12	2.18	Y
	PBS vs 5% β -C-P	44.26	1.00	1.15	0.78	1.68	N
	PBS vs 20% C-P	51.88	5.63	1.28	0.86	1.89	N
	PBS vs RIF alone	51.29	4.05	1.26	0.85	1.87	N
72	PBS	39.95	0.79	–	–	–	–
	PBS vs 20% β -C-P	72.16	1.53	1.8	1.28	2.52	Y
	PBS vs 10% β -C-P	60.21	1.65	1.5	1.06	2.1	Y
	PBS vs 5% β -C-P	45.71	2.56	0.93	0.63	1.39	N
	PBS vs 20% C-P	47.13	3.99	1.17	0.8	1.75	N
120	PBS vs RIF alone	48.77	2.55	1.22	0.82	1.80	N
	PBS	41.49	2.86	–	–	–	–
	PBS vs 20% β -C-P	79.79	1.97	1.91	1.36	2.7	Y
	PBS vs 10% β -C-P	29.67	0.99	0.71	0.5	1.01	N
	PBS vs 5% β -C-P	38.51	1.57	1.37	0.92	2.02	N
120	PBS vs 20% C-P	ND	–	–	–	–	–
	PBS vs RIF alone	ND	–	–	–	–	–
	PBS	35.60	1.21	–	–	–	–
	PBS vs 20% β -C-P	35.60	1.21	1.4	0.98	1.96	Y
	PBS vs 10% β -C-P	49.67	0.93	0.92	0.61	1.37	N
120	PBS vs 5% β -C-P	48.60	1.49	1.48	1	2.21	N
	PBS vs 20% C-P	ND	–	–	–	–	–
	PBS vs RIF alone	ND	–	–	–	–	–

(Continued)

Table 5. (Continued)

Concentration of IL-1 β [pg/ml] in BAL supernatant post-OPA							
Time (h)	Comparison	Mean	SEM	estimate	conf. low	conf. high	Significance
168	PBS	34.01	2.18	–	–	–	–
	PBS vs 20% β -C-P	64.46	1.80	1.89	1.34	2.64	Y
	PBS vs 10% β -C-P	46.73	1.49	1.23	0.83	1.85	N
	PBS vs 5% β -C-P	50.35	7.57	1.49	1.01	2.22	N
	PBS vs 20% C-P	ND	–	–	–	–	–
	PBS vs RIF alone	ND	–	–	–	–	–

A single bolus dose (50 μ L) was administered to mice of either 20% β -C-P, 10% β -C-P, 5% β -C-P, 20% C-P or Rif alone by OPA. BAL was performed and BAL supernatant was analyzed for IL-1 β secretion using an ELISA. Data shown represent the mean \pm SEM; ($n = 4$ to 12). The average effect ratios of the form mean (treatment)/mean (PBS) computed separately for each time was computed separately for each treatment/PBS (and also averaged across all treatments/PBS). These effect ratios were subsequently inferred through their point and interval estimates based on the posterior median and 95% equal-tailed intervals. Statistical significance was measured at the 95% posterior probability level: an effect ratio with 95% posterior probability excluding the value of 1 was deemed statistically significant.

bactericidal small molecule with a short half-life (3 h).^[9] We compared Rif alone administered by gavage with β -C-P nanoparticles or Rif alone administered by OPA. Our results demonstrate β -C-P nanoparticles provide significantly increased amounts of Rif in the BAL of mice, and surprisingly, can provide Rif to the airway space for at least 7 days. This would be a significant clinical advantage for patient compliance. Second, while there is significant Rif found in the BAL after 20% β -C-P nanoparticles administration, serum Rif is non-detectable after 1 day. This is likely due to a rapid burst release of Rif upon administration, followed by slow release, demonstrated by BAL concentrations decreasing over time. Moreover, the amount of Rif detected in BAL after dosing by gavage or OPA is significantly lower whereas, the serum concentrations are higher than β -C-P nanoparticles. This is another advantage of the β -C-P nanoparticles, as the limited serum

concentration would likely lead to reduced side effects. To assess the therapeutic exposure of Rif, the AUC was calculated between 2 and 8 h to avoid making any assumption about the absorption phase and likely t_{max} , and many of the free drug samples had Rif that was below the limit of detection after 8 h. The BAL AUC of the 20% β -C-P nanoparticles is $\approx 64.6x$ free drug gavage (current route of Rif administration); however, the serum AUC of the 20% β -C-P nanoparticles is only 0.54x of the free drug gavage (Table 2). Overall, our PK studies demonstrate that after a single OPA dose of β -C-P nanoparticles to healthy mice, Rif was detected in the cellular fraction of the BAL up to 7 days post-dosing demonstrating sustained Rif release with significantly higher drug exposure in the lung compared to Rif alone administered by both gavage and OPA and reduced systemic exposure.

Mtb infection is known to suppress the proinflammatory response of host cells.^[33] Cytokines act as messengers in the immune system, regulating immune responses, inflammation, and tissue repair during host defense. TNF α , IL-1 β , and IL-6 are particularly crucial in the host's response to *Mtb*, affecting both disease progression and protective immunity.^[34] Studies indicate that blocking TNF α can accelerate TB progression in experimental models.^[34,35] Moreover, TNF α has been associated with immunopathological responses in TB, with its positive or negative effects dependent on dose.^[34,36] Regarding IL-1 β , mice lacking IL-1 β have shown increased susceptibility to *Mtb* infections, underscoring the importance of IL-1 β in host resistance.^[34] Given these insights, our study specifically focused on the effects of nanoparticles on the secretion of TNF α , IL-1 β , and IL-6 from alveolar macrophage (BAL supernatant, cytology demonstrates >97% macrophage in BAL). Our data demonstrated that alveolar macrophage is the primary cell type of uptake following OPA (Supporting Information). Our results demonstrated that all nanoparticles tested induced the release of these cytokines within a range similar to concentrations observed in a TB mouse model after drug treatment.^[34,35,37] Importantly, our findings suggest that nanoparticle administration does not trigger an exaggerated immune response, thus reducing the risk of a cytokine storm, which can lead to severe complications such as respiratory distress, shock, and organ damage.^[38] Furthermore, there were no observed alterations in serum cytokine secretion (data not shown), indicating that nanoparticle administration does not

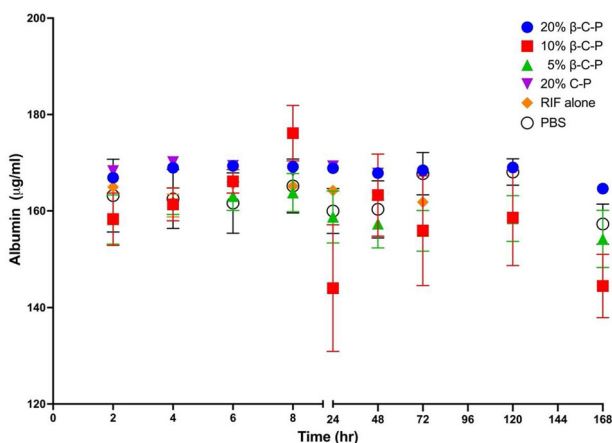


Figure 2. Effect of nanoparticle exposure on albumin concentrations in the BAL supernatant. A single bolus dose (50 μ L) was administered to mice of either nanoparticles 20% β -C-P, 10% β -C-P, 5% β -C-P, 20% C-P or Rif alone by OPA. BAL was performed and BAL supernatant was analyzed for albumin using an ELISA. Data shown represent the mean \pm SEM; ($n = 4$ to 8). Statistical analysis was done using two-way ANOVA followed by Dunnett's multiple comparisons. All data are compared to PBS at respective time points. No significant change occurred in the concentration of albumin in the BAL supernatant at all parameters tested indicating no damage to the alveolar epithelium.

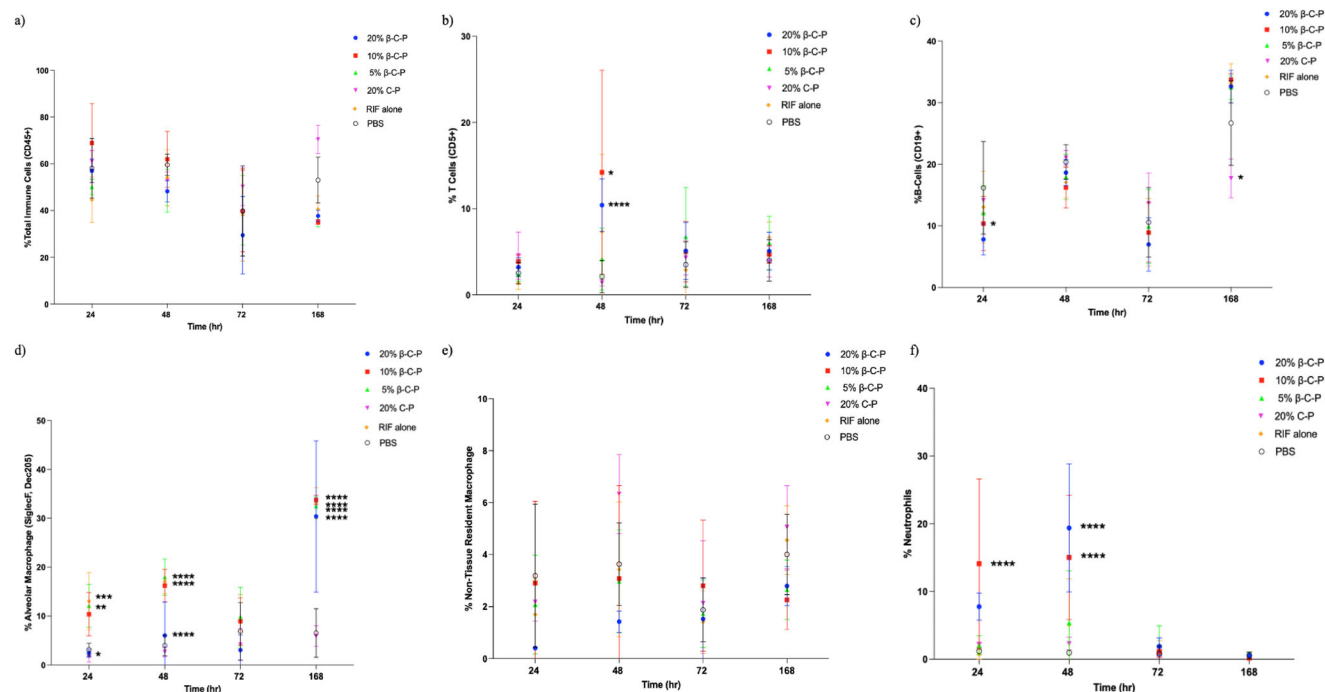


Figure 3. Effect of Nanoparticle Exposure on Immune cell Populations in the Lungs. A single bolus dose (50 μ L) was administered to mice of either nanoparticles 20% β -C-P, 10% β -C-P, 5% β -C-P, 20% C-P or Rif alone by OPA. Lung tissue was collected at 24, 48, 72 h and 7 days post-OPA. Lung tissue was dissociated into single cell suspensions followed by surface marker staining. Data was analyzed by flow Cytometry. Statistical analysis was done using two-way ANOVA followed by Dunnett's multiple comparisons test. All data are compared to PBS at respective time point. Data shown represent the mean \pm SEM; ($n = 8$). a) Total cells, b) T-cells, c) B cells, d) alveolar macrophage, e) proinflammatory cells, f) neutrophils. * = $p < 0.05$; ** = $p < 0.01$; *** = $p < 0.001$; **** = $p < 0.0001$.

provoke sepsis or systemic inflammation. This conclusion is supported by the use of the murine sepsis score, where all mice scored within the normal range across various parameters, including activity level, response to stimuli, posture, respiration rate and quality, and overall appearance.^[39,40] Additionally, analysis of albumin accumulation in the interstitial and alveolar spaces revealed no evidence of damage to blood vessels or the alveolar epithelium. These findings align with previous data on albumin levels in BAL in mice and indicate that β -C-P nanoparticles do not induce damage to the alveolar epithelium, thereby minimizing potential physiological consequences in the lungs and systemically.

Given that we were delivering a foreign substance, a nanoparticle, to the lungs, we hypothesized that the alveolar macrophage population, the primary site of *Mtb* infection,^[33] would be modulated following a single OPA bolus dose of β -C-P or C-P nanoparticles to the pulmonary airspaces. Alveolar macrophages are plastic and function to regulate homeostatic conditions in the lungs, thereby reducing lung inflammation and tissue injury.^[41,42] We found a significant increase in the alveolar macrophage population at 24, 48, and 168 h for 20% β -C-P and 10% β -C-P, and at 48 and 168 h for 5% β -C-P. Interestingly, C-P nanoparticles had no effect on the alveolar macrophage population. This highlights the role of the immunostimulatory ligand β -glucan on the surface of the nanoparticle in modulation of the immune response in alveolar macrophage. Understanding how alveolar macrophages interact in their environment and respond to the nanoformulation is crucial for translating this immunos-

timulatory nanoparticle to the clinic. The monocyte-derived macrophage (proinflammatory) population has been shown to migrate to the alveoli and develop features similar to alveolar macrophages.^[41,42] This may occur following a single nanoparticle administration. However, we did not observe a change in the overall proinflammatory macrophage population, which is reflective of monocyte-derived macrophages. Additionally, alveolar macrophages can exhibit immunosuppressive activities, potentially reducing lung inflammation and injury. The observed increase in alveolar macrophage may be aimed at limiting tissue damage.

In addition to alveolar macrophage, several other immune cells play an important role in response to injury in the lung, this includes innate and adaptive immune cells such as neutrophils and T-cells. β -C-P nanoparticles transiently increased the T-cell population. CD4+ T-cells are required for immunity to *Mtb*.^[43] This transient increase may increase the adaptive immune response against *Mtb*. Similarly, a transient increase occurred in the neutrophil population after exposure to β -C-P nanoparticles. Typically, healthy lungs maintain a low percentage of neutrophils, around 0.5%. In instances involving LPS, murine neutrophil populations have been observed to surge to 90%.^[44,45] While there was an initial increase in neutrophils, it resolved within 72 h. Recruitment of neutrophils by β -C-P nanoparticles may be advantageous, as it is well-documented that neutrophils play a pivotal role in the elimination of *Mtb*.^[46,47]

In conclusion, our study underscores the potential of β -glucan-CS-PLGA nanoparticles as a promising immunostimulatory

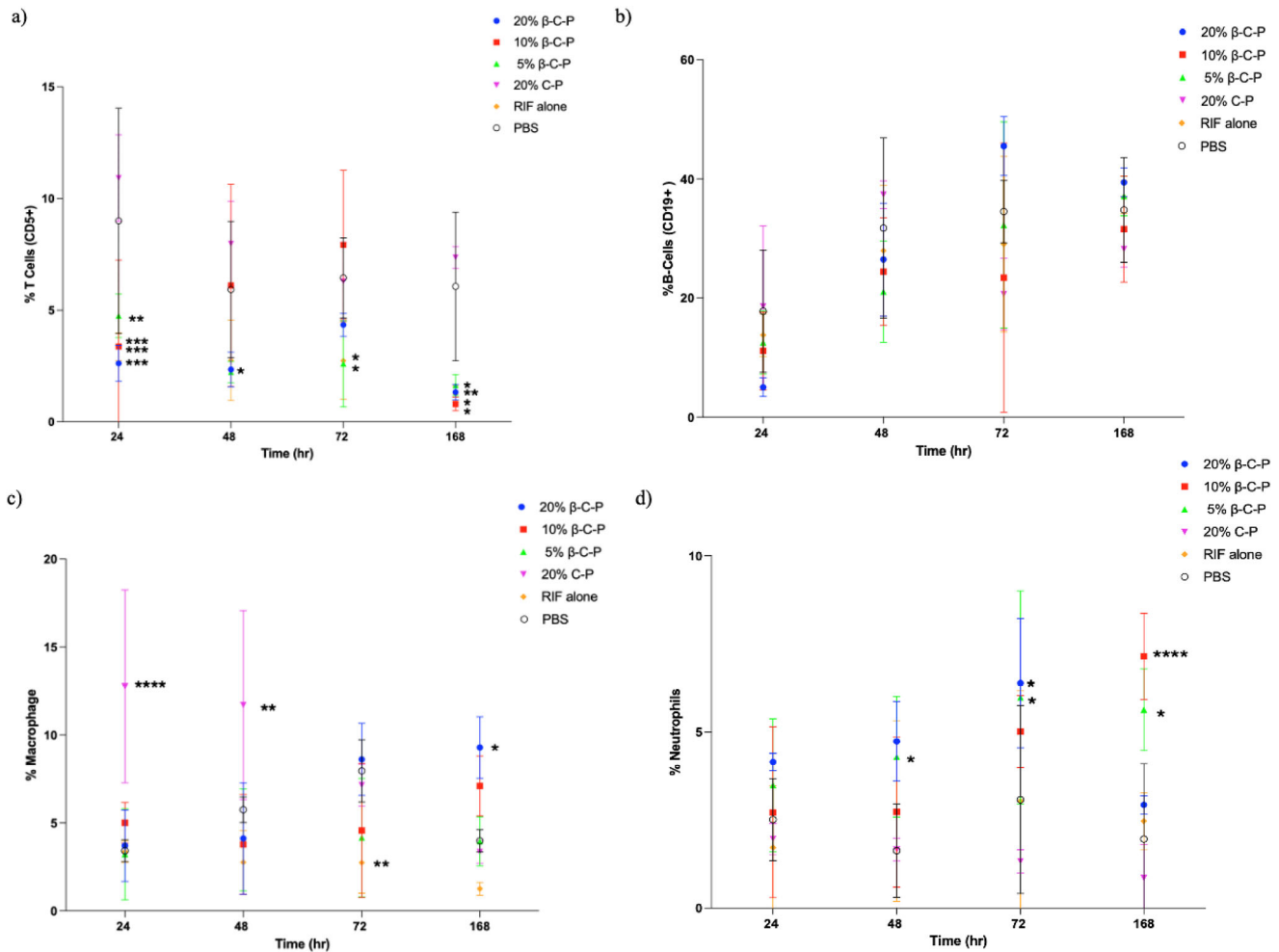


Figure 4. Effect of nanoparticle exposure on immune cell population in the spleen A single bolus dose (50 μ L) was administered to mice of either nanoparticles 20% β -C-P, 10% β -C-P, 5% β -C-P, 20% C-P or Rif alone by OPA. The spleen was collected at 24, 48, 72 h and 7 days post OPA. The spleen was dissociated into single cell suspensions followed by surface marker staining. Data was analyzed by flow Cytometry. Data shown represent the mean \pm SEM; ($n = 8$). Statistical analysis was done using two-way ANOVA followed by Dunnett's multiple comparisons test. All data are compared to PBS at respective time points. a) B cells, b) T cells, c) Macrophage, d) Neutrophils. * = $p < 0.05$; ** = $p < 0.01$; *** = $p < 0.001$; **** = $p < 0.0001$.

adjunct for TB treatment. Pharmacokinetic investigations reveal the sustained release properties of Rif in vivo, extending over a week. Furthermore, comprehensive analysis indicates stimulation of the innate immune system, as evidenced by cytokine profiling, while concurrently revealing no detrimental effects on the alveolar epithelium, as indicated by histological examination and albumin lung leak assessment. These findings collectively establish a strong foundation for the development of a novel adjuvant immunotherapy approach for TB. Looking forward, we envision the translation of this therapeutic modality as an inhalational adjuvant for TB management, offering a more pragmatic and feasible drug delivery strategy for patients. By transitioning to a once-per-week dosing regimen, this approach holds the potential to surmount the challenges associated with daily administration and mitigate dose-limiting side effects. Currently, ongoing investigations are underway to further assess the efficacy of these nanoparticles in a mouse model of TB. Through continued research and refinement, we aim to advance this innovative therapeutic paradigm toward clinical translation, ultimately ad-

ressing the pressing need for more effective and patient-friendly treatments for TB.

Supporting Information

Supporting Information is available from the Wiley Online Library or from the author.

Acknowledgements

H.L.K. and M.T. contributed equally to this work. Research reported in this publication was supported by the National Institute of Allergy and Infectious Disease of National Institutes of Health under award number 1R01AI129649; 1R21AI179228; the National Center for Advancing Translational Sciences of the National Institutes of Health under award number UL1TR001412, the National Institutes of Health under award number KL2TR001413 to the University at Buffalo The content is solely the responsibility of the authors and does not necessarily represent the official views of the NIH.

Conflict of Interest

The authors declare no conflict of interest.

Data Availability Statement

The data that support the findings of this study are available from the corresponding author upon reasonable request.

Keywords

alveolar macrophage, beta-glucan, nanoparticles, rifampin, tuberculosis

Received: February 8, 2024

Revised: June 11, 2024

Published online: July 5, 2024

- [1] E. Luke, K. Swafford, G. Shirazi, V. Venketaraman, *Front Biosci (Schol Ed)* **2022**, *14*, 6.
- [2] *Global Tuberculosis Report 2023*, Geneva: World Health Organization, **2023**.
- [3] Z. Z. Sultana, F. U. Hoque, J. Beyene, M. d. Akhlak-Ul-Islam, M. d. H. R. Khan, S. Ahmed, D. H. Hawlader, A. Hossain, *BMC Infect. Dis.* **2021**, *21*, 51.
- [4] M. D. Iseman, *Eur. Respir. J. Suppl.* **2002**, *36*, 87s.
- [5] A. Matteelli, S. Lovatti, A. Sforza, L. Rossi, *Int. J. Infect. Dis.* **2023**, *130*, S43.
- [6] E. Pontali, M. C. Raviglione, G. B. Migliori, *Eur. Respir. Rev.* **2019**, *28*, 190035.
- [7] A. Dube, J. L. Reynolds, W.-C. Law, C. C. Maponga, P. N. Prasad, G. D. Morse, *Nanomedicine* **2014**, *10*, 831.
- [8] H. L. Kutscher, G. D. Morse, P. N. Prasad, J. L. Reynolds, *Pharm. Res.* **2019**, *36*, 44.
- [9] G. Acocella, *Rev Infect Dis* **1983**, *3*, S428.
- [10] N. Dalonso, G. H. Goldman, R. M. Gern, *Appl. Microbiol. Biotechnol.* **2015**, *99*, 7893.
- [11] X. Zheng, S. Zou, H. Xu, Q. Liu, J. Song, M. Xu, X. Xu, L. Zhang, *Carbohydr. Polym.* **2016**, *148*, 61.
- [12] L. Yang, L. Chaves, H. L. Kutscher, S. Karki, M. Tamblin, P. Kenney, J. L. Reynolds, *Front. Bioeng. Biotechnol.* **2023**, *11*, 1095926.
- [13] G. Hetland, P. Sandven, *FEMS Immunol. Med. Microbiol.* **2002**, *33*, 41.
- [14] S. J. C. F. M. Moorlag, N. Khan, B. Novakovic, E. Kaufmann, T. Jansen, R. van Crevel, M. Divangahi, M. G. Netea, *Cell. Rep.* **2020**, *31*, 107634.
- [15] L. Shao, S. Shen, H. Liu, *Front Bioeng Biotechnol* **2022**, *10*, 941077.
- [16] F. Makita-Chingombe, H. L. Kutscher, S. L. DiTursi, G. D. Morse, C. C. Maponga, *J Drug Deliv* **2016**, *2016*, 3810175.
- [17] I. Rather, N. Shafiq, J. Shukla, G. Kaur, S. Pandey, R. K. Bhandari, A. K. Pandey, B. R. Mittal, G. K. Khuller, N. Sharma, S. Malhotra, *Br. J. Clin. Pharmacol.* **2023**, *89*, 3702.
- [18] Q. Liang, H. Xiang, X. Li, C. Luo, X. Ma, W. Zhao, J. Chen, Z. Tian, X. Li, X. Song, *Int. J. Nanomedicine* **2020**, *15*, 7491.
- [19] S. K. Jain, Y. Gupta, L. Ramalingam, A. Jain, A. Jain, P. Khare, D. Bhargava, *PDA J. Pharm. Sci. Technol.* **2010**, *64*, 278.
- [20] R. Pandey, G. K. Khuller, *Tuberculosis (Edinb)* **2005**, *85*, 227.
- [21] T. Gumbo, A. Louie, M. R. Deziel, W. Liu, L. M. Parsons, M. Salfinger, G. L. Drusano, *Antimicrob. Agents Chemother.* **2007**, *51*, 3781.
- [22] B. W. Neun, E. Cedrone, T. M. Potter, R. M. Crist, M. A. Dobrovolskaia, *Molecules* **2020**, *25*, 3367.
- [23] R. Alluri, H. L. Kutscher, B. A. Mullan, B. A. Davidson, P. R. Knight, *J. Vis. Exp.* **2017**, *26*, e54700.
- [24] T. Jaki, M. J. Wolfsegger, *Pharmaceutical Statistics* **2011**, *10*, 284.
- [25] A. Gelman, J. B. Carlin, H. S. Stern, D. B. Dunson, A. Vehtari, D. B. Rubin, *Bayesian Data Analysis*, 3rd ed, Chapman and Hall/CRC, New York **2013**.
- [26] B. Goodrich, J. Gabry, I. Ali, S. Brilleman, 'Rstanarm: Bayesian Applied Regression Modeling via Stan, <https://mc-stan.org/rstanarm/> (accessed: **2022**)
- [27] H. Wickham, M. Averick, J. Bryan, W. Chang, L. McGowan, R. François, G. Grolemund, A. Hayes, L. Henry, J. Hester, M. Kuhn, T. Pedersen, E. Miller, S. Bache, K. Müller, J. Ooms, D. Robinson, D. Seidel, V. Spinu, K. Takahashi, D. Vaughan, C. Wilke, K. Woo, H. Yutani, *J. Open Source Software* **2019**, *4*, 1686.
- [28] V. Arel-Bundock, N. Greifer, A. Heiss, *J. Stat. Softw.* **2023**.
- [29] L. L. I. J. Booyesen, L. Kalombo, E. Brooks, R. Hansen, J. Gilliland, V. Gruppo, P. Lungenhofer, B. Semete-Makokotlela, H. S. Swai, A. F. Kotze, A. Lenaerts, L. H. du Plessis, *Int. J. Pharm.* **2013**, *444*, 10.
- [30] S. Malathi, S. Balasubramanian, *J. Biomed. Nanotechnol.* **2011**, *7*, 150.
- [31] M. Tukulula, L. Gouveia, P. Paixao, R. Hayeshi, B. Naicker, A. Dube, *Pharm. Res.* **2018**, *35*, 111.
- [32] B. E. Betz, A. K. Azad, J. D. Morris, M. V. S. Rajaram, L. S. Schlesinger, *Microb. Pathog.* **2011**, *51*, 233.
- [33] F. Ahmad, A. Rani, A. Alam, S. Zarin, S. Pandey, H. Singh, S. E. Hasnain, N. Z. Ehtesham, *Front. Immunol.* **2022**, *13*, 747799.
- [34] A. M. Cooper, K. D. Mayer-Barber, A. Sher, *Mucosal Immunol.* **2011**, *4*, 252.
- [35] Y. V. Cavalcanti, M. C. Brelaz, J. K. Neves, J. C. Ferraz, V. R. Pereira, *Pulm. Med.* **2012**, *2012*, 745483.
- [36] P. Sankar, B. B. Mishra, *Front. Immunol.* **2023**, *14*, 1260859.
- [37] M. Maiga, B. A. Ahidjo, M. C. Maiga, L. Cheung, S. Pelly, S. Lun, F. Bougoudogo, W. R. Bishai, *EBioMedicine* **2015**, *2*, 868.
- [38] M. J. Delano, P. A. Ward, *Immunol. Rev.* **2016**, *274*, 330.
- [39] B. Shrum, R. V. Anantha, S. X. Xu, M. Donnelly, S. M. Maeryfar, J. K. McCormick, T. Mele, *BMC Res. Notes* **2014**, *7*, 233.
- [40] M. M. Sulzbacher, L. M. Sulzbacher, F. R. Passos, B. L. E. Bilibio, K. de Oliveira, W. F. Althaus, M. N. Frizzo, M. S. Ludwig, I. B. M. Da Cruz, T. G. Heck, *Biomed Res. Int.* **2022**, *2022*, 1.
- [41] B. Allard, A. Panariti, J. G. Martin, *Front. Immunol* **2018**, *9*, 1777.
- [42] F. Hou, K. Xiao, L. Tang, L. Xie, *Front. Immunol* **2021**, *12*, 753940.
- [43] S. Sakai, K. D. Mayer-Barber, D. L. Barber, *Curr. Opin. Immunol.* **2014**, *29*, 137.
- [44] L. Van Hoecke, E. R. Job, X. Saelens, K. Roose, *J. Vis. Exp.* **2017**, *4*, e55398.
- [45] V. D. Giacalone, C. Margaroli, M. A. Mall, R. Tirouvanziam, *Int. J. Mol. Sci.* **2020**, *21*, 851.
- [46] I. V. Lyadova, *Mediators Inflammation* **2017**, *2017*, 8619307.
- [47] J. N. Hilda, S. Das, S. P. Tripathy, L. E. Hanna, *Innate Immun.* **2020**, *26*, 240.